Field and UV induced electron emission properties of doped SnO_2 and In_2O_3 thin layers

Jadwiga Olesik, Zygmunt Olesik and Michael J. Malachowski*

Abstract

This paper describes a series of experiments involving the study of electron emission (with and without illumination) from electrically polarised cells comprising thin, transparent and conductive Sn doped In_2O_3 (ITO) layers deposited onto both surfaces of thin glass plates. The exponential dependence of emission frequency on applied voltage can be attributed to well-known effects and this has been confirmed using spectral decomposition. Approximately 80% of emitted electrons have energies up to 10 eV. Photoinduced optical second harmonic (SHG) has also been observed.

Introduction

Malter's effect [1]. is concerned with the investigation of the secondary electron emission phenomenon [2] with an inner electric field in the sample. In our studies the sample was a microscope cover glass with semiconducting films of indium tin oxide evaporated on both sides. The film, where the polarizing voltage U_{pol} was applied was the field electrode, whereas the opposite film was the emitting layer. By applying an appropriate voltage, U_{pol} to the layers one may create an inner electric field of a given direction and value.

A four-grid retarding potential analyzer makes it possible to investigate changes in the coefficient δ when all the grids are short-circuited and grounded. The energy spectra of secondary electrons change in a characteristic way with increasing negative value of the U_{pol} voltage (which creates an electric field in a sample): for first maximum the primary peak shifts to the lower energies, for second maximum electrons of energy greater than primary are detected [2]. Electrons of such energies have also been detected by Ibach [3]. The values of U_{pol} at which the characteristic changes in the energy spectra occur, are different dependent on the primary electron energy.

The above results allow the development of a model for SEE induced by the electric field. This model is based on the assumptions that the U_{pol} voltage forms two zones, in the conducting layer, one of enhanced and the other one of depleted of free electrons and the value of U_{pol} influences the width of the zones, penetration depth of primary electrons and outcome depth of secondary electrons. When a primary electron penetrates the enhanced zone, it may in most cases cause an increase of concentration of conduction electrons, with possible appearance of so-called hot electrons. The two phenomena may occur simultaneously; electrons in the depleted layer are released into the conduction band or, as a result of retardation in the electric field, it changes its direction or even produces secondary electrons in cascade multiplication. An investigation of the electron emission with the internal field but without a primary beam was also performed, due to complexity of the interaction between the primary beam and the internal field.

* Institute of Physics, Pedagogical University, Armii Krajowej 13/15, 42-201 Czestochowa, Poland

Experiment

Two conducting films were evaporated on the both sides of a microscopic cover glass 16x16x0.2 mm. One film, In_2O_3:Sn (ITO) of the thickness about 10nm was the emitting surface. The other, (1μm) was polarized in order to create an internal field (field electrode). The surface resistance was varied within 1-50 Ω/cm. Coatings on glass with highly transparent conductive oxide films (TCO) are performed mostly by using indium tin oxide layers (ITO) [4 - 9]. The measurements were performed at a pressure of about $2x10^{-6}$ Pa. The sample as well as the electron energy analyzer and electron multiplier were placed in vacuum. Applying polarizing voltage U_{pol}, within the interval from -2000 V to 0 V, created at the field electrode an internal field, which favored electron emission into vacuum. The schematic diagram of the apparatus is shown in figure 1.

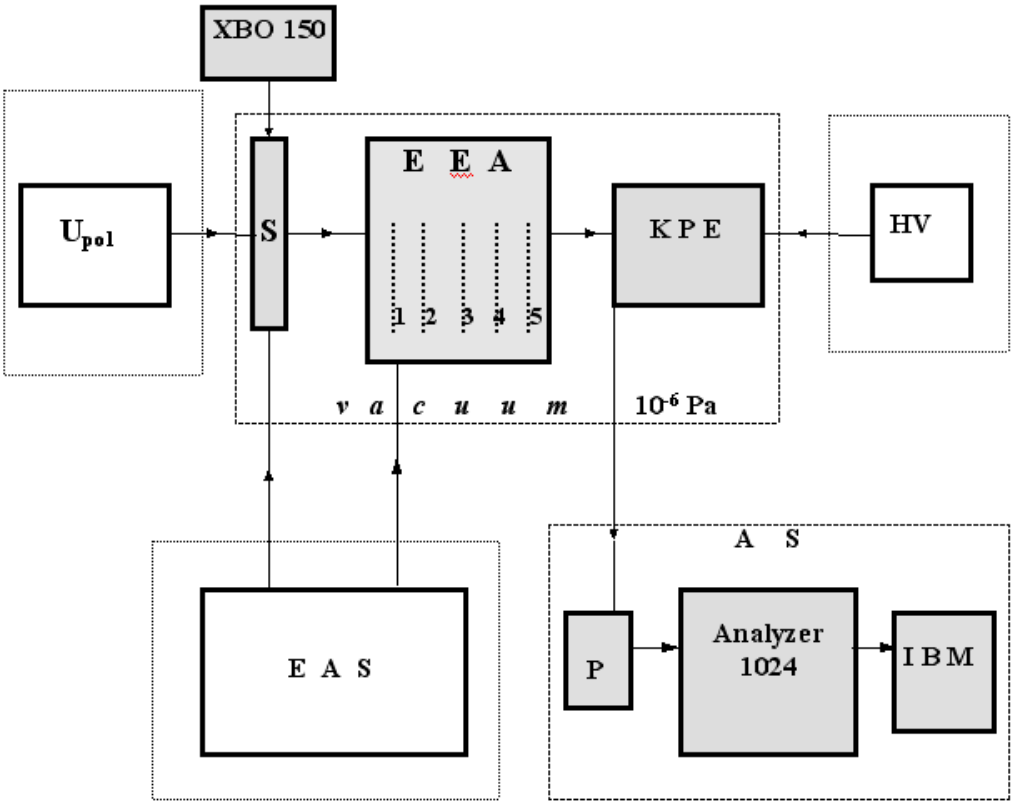

Figure 1. Schematic diagram of the electronic measuring system:
S - sample, EEA - electron energy analyzer (1,2,3,4,5- grids), KPE - channeltron KPE (∅7) 405, HV - channeltron supply (HV = 2.9 kV), U_{pol} - polarizing voltage supply, EAS - energy analyzer supply (U_a, U_p), AS - pulse acquisition and description system (P-preamplifier, Tristan 1024- multichannel pulse amplitude analyzer, IBM-computer), XBO 150 - quartz lamp.

Results

1. Spectral decomposition on Gaussians

We used the program *Gauss* for decomposition of the obtained function N(U) = f(U) on the component functions using the non-linear regression method. We have found that after decomposition process, the observed spectra did not always had a single maximum, sometimes a double maximum curve occurred, which corresponds to a single-electron or two-electron impulse respectively. The principle of minimal number of the maxima was

used for decomposition process. Exemplary amplitude spectra of voltage impulses after decomposition on the Gaussian components are presented in figure 2. The ordinate gives the number of pulses at a particular analyzer channel and the channel number converted into the pulse amplitude in mV, are given on the abscissa. A single spectrum was recorded during 500s. They were obtained at various U_{pol} for both illuminated and not illuminated samples [10 - 11]. As one can see from figure 2, the N (U) = f (U) dependence can be approximately described by a Gauss function. The approximation is better or worse depending on U_{pol} and on whether the sample has been illuminated or not. It was assumed that if the amplitude spectrum can be described by a single Gaussian curve then electrons come into the multiplier in time intervals determined by the time resolution of the electron multiplier (maximum pulse count rate – 10^5 cps).

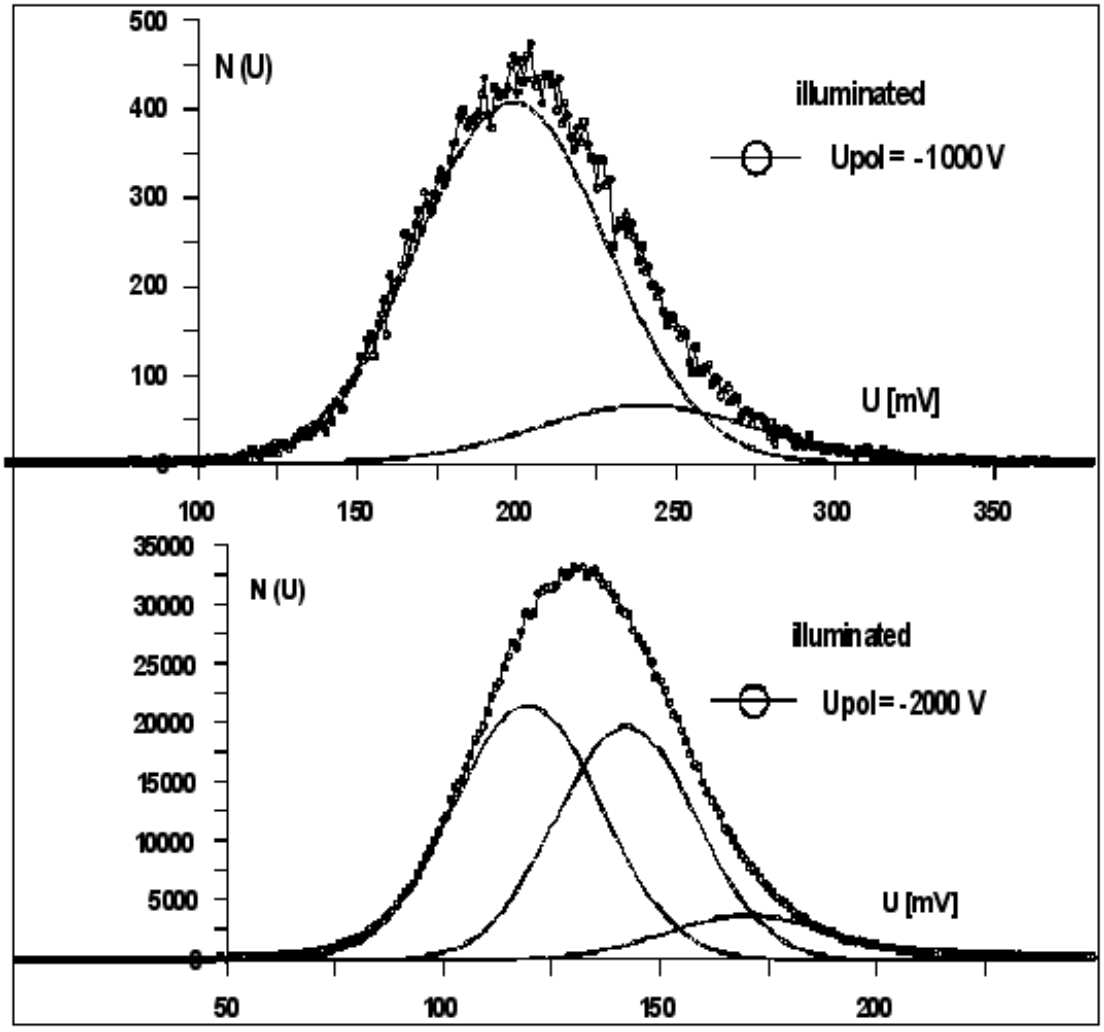

Figure 2. Exemplary pulse amplitude spectra and their decomposition into Gaussians for an illuminated sample.

However, if the spectrum must be approximated by more than one Gaussian curve, then more than one electron must come to the multiplier in the resolution time (beside those electrons, which come as single in resolution time). Using this hypothesis the experimentally obtained spectra were decomposed into Gaussian curves. The proposed way of spectra interpretation is based on decomposition of the complex envelope of spectra into separate peaks and summation of the spectra. This was computed using the non-linear regression method, which also allowed the determination of best-fit parameters.

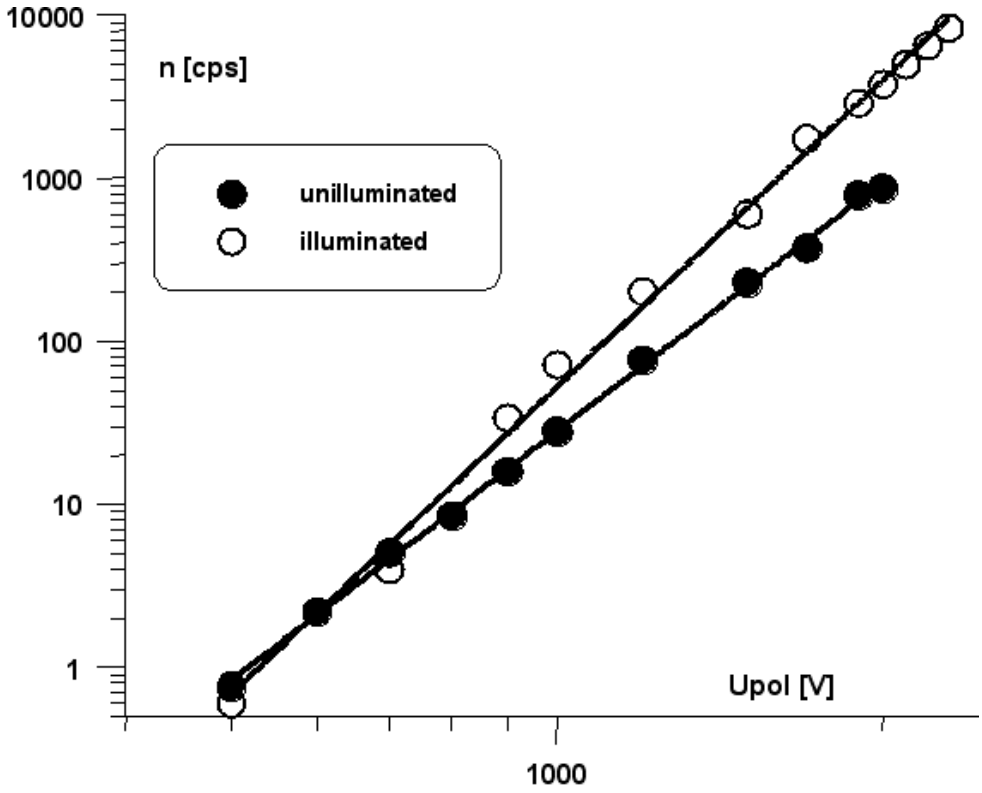

Figure 3. Logarithmic plot of count frequency as function of negative polarizing voltage.

2. Emission and photoemission yield

On the basis of the obtained amplitude spectra we can see that with increasing U_{pol} the number of counts in a given registration time is growing. In order to check the more closely, we measured the number of pulses recorded in frequency of counts, *n* in cps. With increasing U_{pol} (field strength in a sample) the count frequency *n* grows monotonically. Fig. 3 shows the frequency *n* as a function of voltage U_{pol} after illumination and without illumination of the sample. For non-illuminated samples this dependence can be described by the equation:

$$n = k\,(U_{pol})^5$$

For illuminated samples the $n = f(U_{pol})$ dependence can be described by:

$$n = k\,(U_{pol})^6$$

3. Energy distributions of electrons

We attempted to evaluate the energy of emitted electrons using the retarding field method. It is obvious that the number of counts in the channels of the pulse analyzer should decrease with decreasing value of the analyzing voltage U_a. Figure 4 shows that frequency *n* decreases rapidly with increasing the negative voltage U_a (up to about 10 V). It means that the energy of most emitted electrons is within the range of 0 to 10 eV. Although possible, the appearance of high-energy electrons, having energy above 10 eV, has a small probability.

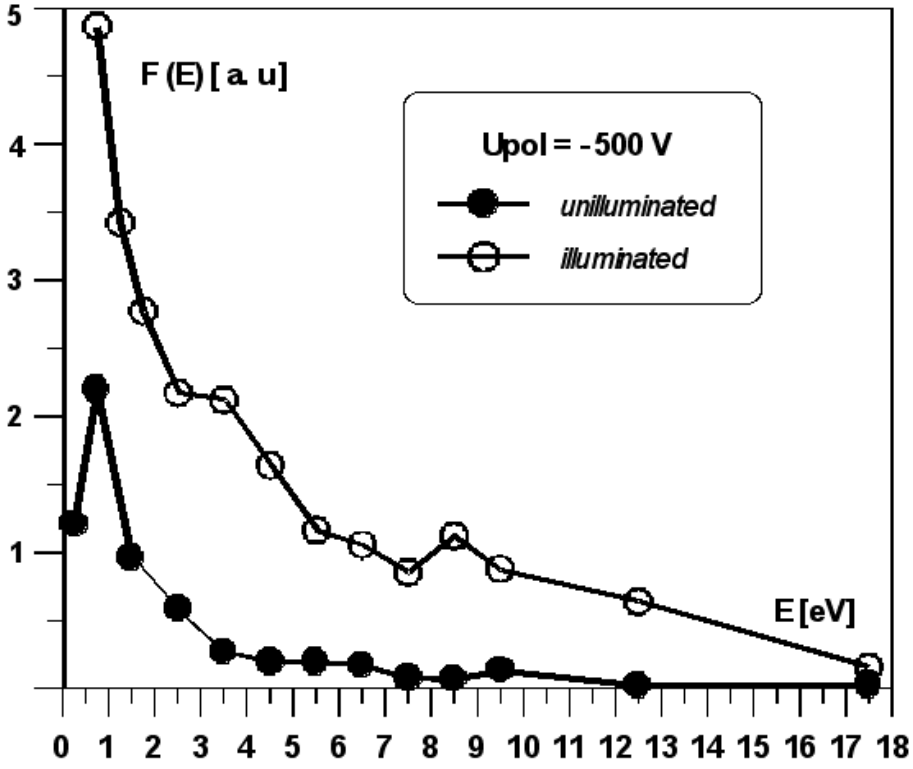

Figure 4. Count frequency *n* as a function of analyzing voltage V_a.

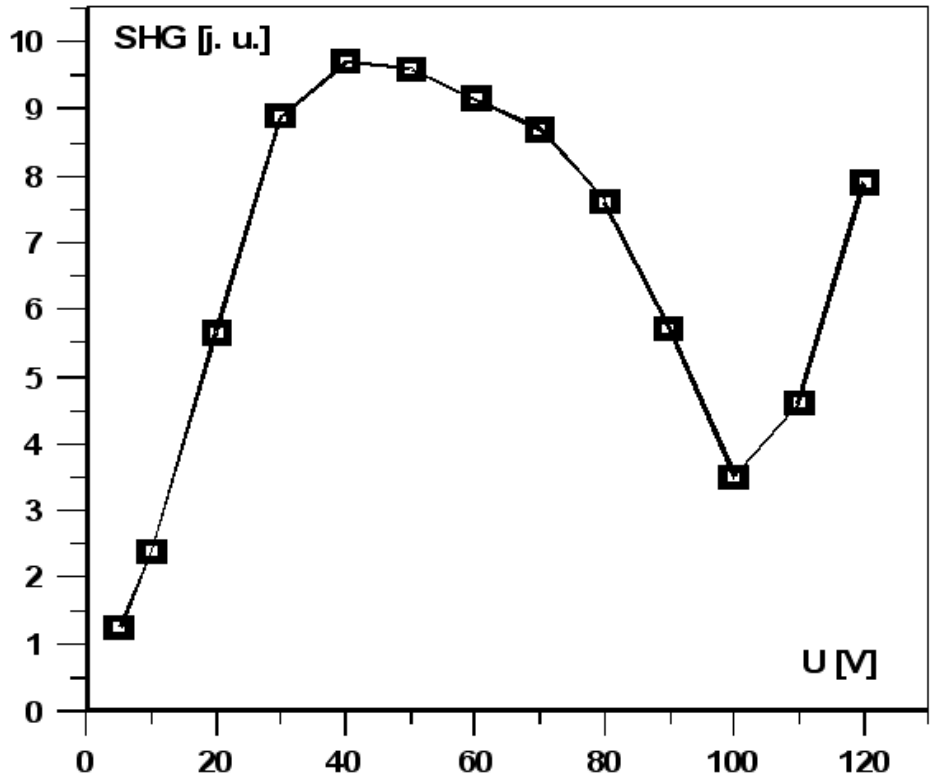

Figure 5. Photoinduced SHG intensity as function of polarizing voltage U at 77K.

4. Nonlinear effects

The SHG signal achieves its maximum value at 50V followed by a slow decrease that reflects a possible contribution of two non-equilibrium metastable oxygen states (Fig. 5).

Therefore, there appears to be a possibility to operate the SHG reflected signal using only the internal applied electric field. To estimate a density of quantum states, electron states and proper optical transitions for the Sn-O clusters, before and after the photoinduced processes have been studied [12 -13].

Conclusions

1. The applied voltage creates the field in the complex emitter (ITO layer on the glass substrate) and this results in electron emission into vacuum. The average field inducing the emission should be of the order 1 MV/m.
2. The effect of electric field induced electron emission (FIEE) occurs due to processes resulting in electron gas heating: Gunn effect, impact and electrostatic ionization, tunnel effect as well as field induced surface potential barrier lowering. The mechanism resembles the emission effect in the emitter with negative electron affinity.
3. FIEE yield increases with increasing applied voltage U_{pol},creating the electric field in the sample. The $n = f(U_{pol})$ dependence can be described by $n \sim (U_{pol})^5$.
4. Ultraviolet radiation together with applied electric field results in an electron emission effect called field induced photoemission (FIPE).
5. FIPE yield increases exponentially with the increase of U_{pol}. Dependence $n = f(U_{pol})$ can be described by $n \sim (U_{pol})^6$. Emission yield of the FPE effect was found to be several time higher than the emission yield of IFEE process (particularly for higher U_{pol}).
6. Spectra decomposition was based on the rule of minimization of peak number. If the electrons come into vacuum according with a pulse count rate then the amplitude spectrum can be described by a single Gaussian. However, if the spectrum must be approximated by more than one Gaussian, then it is assumed that more than one electron is emitted within the multiplier resolution time.
7. Electrons generated through the FIPE and IFEE processes depending on the applied voltage U_{pol} can be created in: the surface region of the ITO layer, the interface region of glass-ITO and by double electron photoemission.
8. Among the electrons emitted as a result of FIPE and IFEE effects, about 80% were found to have energy not exceeding 10 eV, while the maximum of energy spectrum occurs at energy of 1 eV.
9. Second harmonic generation (SHG) was detected in glass-ITO systems. The intensity of the SHG signal reaches a maximum at about 50V (at low temperature). The main role in the observed phenomena play the interaction between the tetrahedral SnO_4 and Sn-O clusters of the glass substrate.
10. During the study of emission effects instabilities of the Malter type were encountered, mainly in the films of island structure of dimension about 10nm.

In conclusion we should mention that the above described electron emission model is rather of qualitative character. In order to support our conclusions we are starting to use the TLM numerical method to simulate the observed effects. We believe that amongst others things, the TLM solution of the Laplace equation should be useful in determining the field distribution within the sample.

References

1. L. Malter, *Thin film field emission*, Phys. Rev. **50** (1936) 48-50

2. J. Olesik and B. Calusinski, *Influence of an internal electric field in a sample on the secondary electron emission phenomenon*, Thin Solid Films **238** (1994) 271-275

3. H. Ibach, *Surface vibrations of silicon detected by low-energy electron spectroscopy* Phys. Rev. **27** (1971) 253-255

4. S. Schiller, U. Heising, C. Korndorfel, G. Beister, J. Reschke, K. Steinfelder, J. Strumpfel, *Reactive d.c. high rate sputtering as production technology*, Surf. Coat. Techn., **33** (1987) 405-412

5. M. Saif, H. Patel, H. Memarian, *Overview on transparent conductive films*, Proc. 10th Int. Conf. On Vacuum Web Coating, Fort Lauderdale, (ed. R. Bakish), pp. 285-295, 1996.

6. M. Bender, W. Seeling, C. Daube, H. Frankenberger, B. Ocker, J. Stollenwerk, *Dependence of oxygen flow on optical and electrical properties of DC-magnetron sputtered ITO films*, Thin Solid Films **326** (1998) 72-80

7. M. Orita, H. Tanji, *Mechanism of electrical conductivity of transparent $InGaZnO_4$*, Phys. Rev. B, **61**, (2000) 1811-1816

8. K. Zakrzewska, E. Leja, *The electrical and optical properties of $CdIn_2O_4$ thin films prepared by dc reactive sputtering*, Vacuum **36** (1986) 485-487

9. E. Leja, *Fabrication and Electrical Properties of Transparent Oxide Layers of type SnO_2 and In_2O_3* , **55**, AGH Kraków, 1982 (in Polish).

10. J. Olesik, B. Calusinski, Z. Olesik, *Electron emission phenomena controlled by a transverse electric field in compound emitters* SPIE **2877** (1996) 198-206

11. J. Olesik, M. Ma_achowski, Z. Olesik, *Some optoelectronic properties controlled by an electric field in the glasses coated by thin oxide films* SPIE **3743** (1999) 203-210

12. B. Sahraoui, I.V. Kityk, X. N. Phu, P. Hudhomme, A, Gorgues, *Influence of hydrostatic pressure and temperature on two-photo absorption of a C_{60}-2-thioxo-2.3-dithiole cycloadduct* Phys. Rev. **59B** (1999) 9229-9238

13. Z. Olesik, I.V. Kityk, J. Kasperczyk, J. Olesik, A. Mefleh, *Photoinduced effects in silicon glass coated by In_2O_3-Sn thin layer* Thin Solid Films **358** (2000) 114-121